Drag of Spheroid-Cone Shaped Airship

Graham E. Dorrington*
Queen Mary, University of London, London, England E1 4NS, United Kingdom

Drag coefficients of streamlined bodies and complete airships are compared to confirm some general trends. Data obtained from flight testing an electrically powered, helium-filled, dirigible balloon with a spheroid-cone hull form are analyzed. Wind-tunnel tests indicate that placing a cone behind a sphere reduces its drag coefficient by about 50%, but flight-test data suggest the drag coefficient of the spheroid-cone airship is relatively high. The influence of atmospheric turbulence and nonsteady flow effects are discussed.

Nomenclature

A	=	acceleration modulus
a, b	=	constants used in Eq. (8)
C_{DV}	=	volumetric drag coefficient, defined by Eq. (1)
C_{DVH}	=	Hoerner's formula for C_{DV}, defined by Eq. (2)
C_{decel}	=	effective drag coefficient during deceleration, defined by Eq. (6)
C_F	=	skin friction coefficient
D	=	drag force, N
d_{max}	=	maximum diameter of hull/body, m
F	=	thrust, N
k_x	=	inertia (added mass) coefficient in forward flight direction
L	=	length of hull/body on major axis, m
L_{decel}	=	deceleration parameter, m
M	=	mass, kg
N	=	ratio C_{DVtot}/C_{DVH}
P	=	installed engine/motor power, W
p_m	=	power-to-mass ratio of propulsion system
Re	=	Reynolds number based on hull/body length, $\rho U L / \mu$
r	=	radius from hull center, m
s	=	distance, m
t	=	time, s
U	=	forward velocity, m/s
u_F	=	thrust decay constant, m/s
V	=	volume of hull or body, m³
η_p	=	propulsive efficiency, $F_i U / P = F_{tot} U / P_{tot}$
θ	=	angle from longitudinal centerline through hull
λ	=	fineness ratio of hull, L / d_{max}
μ	=	ambient air viscosity, kg·m²/s
ρ	=	ambient atmospheric density, kg/m³

Subscripts

He	=	helium gas
i	=	ith motor/engine
model	=	wind tunnel model of bare hull or equivalent axisymmetric body
prop	=	propulsion system
tot	=	total, whole (full-scale) airship in flight
∞	=	infinitely far upstream

Introduction

MOST past and existing airships have been designed with streamlined hull forms based on prolate ellipsoids, or similar

*Lecturer, Aerospace Design, Department of Engineering, Mile End Road; g.dorrington@qmul.ac.uk.

bodies of revolution, to reduce hull drag. Alternative lighter-than-air vehicle forms, for example, lenticular shapes, have been developed, but they represent a minority and are not dealt with herein. To minimize the drag of a streamlined hull/body, a prevailing notion is that its major axis length L should be about 4–8 times its maximum diameter d_{max}. In practice, however, the selection of hull fineness ratio, $\lambda = L/d_{max}$, emerges from the consideration of many different design factors. For a given hull volume V, it does not necessarily follow that the optimum design would be one that minimizes the volumetric drag coefficient defined by

$$C_{DV} = D / \left(\tfrac{1}{2} \rho U^2 V^{\frac{2}{3}} \right) \tag{1}$$

where D is the drag force during cruise (assumed to be steady and parallel to the hull major axis), U is the airship's cruise velocity (also assumed to be parallel to the major axis), and ρ is the ambient density. One reason for this is that hull mass will increase with hull surface area, and the designer is often interested in maximizing disposable load. Hence, it is often beneficial to select a value of λ that is lower than the value at which minimum C_{DV} occurs. Before this matter is expanded on further, as well as discussing particular design examples, it is worthwhile reviewing the dependence of C_{DV} on λ.

Drag Coefficients

Drag Coefficients of Streamlined Bodies

Hoerner[1] offered some empirically derived formulas that are now well known and often used in preliminary design studies. Whereas the formulas appear to be crude extrapolations, they actually give reasonable approximations for the drag coefficients of streamlined bodies of revolution, in incompressible flows, over a wide range of λ. The formula for the volumetric drag coefficient is

$$C_{DV} \cong C_{DVH} = C_F \left(4\lambda^{\frac{1}{3}} + 6\lambda^{-\frac{7}{6}} + 24\lambda^{-\frac{8}{3}} \right) \tag{2}$$

where C_F is the (turbulent) skin-friction coefficient of an equivalent flat plate, which is a function of the Reynolds number Re based on the same length L. In the range of interest, a good approximation is

$$C_F = 0.455 / (\log_{10} Re)^{2.58} \cong 0.045 / Re^{\frac{1}{6}} \tag{3}$$

Wind-tunnel test data[2−12] for various axisymmetric bodies (with polygonal as well as circular cross sections) in the range $1 < \lambda < 10$ are presented in Table 1. The predictive success of Eq. (2) appears to be extremely good in a few cases. For example, using data from a test[7] on a 1:180 scale model of the bare R101 rigid-airship hull at $Re \cong 49 \times 10^6$, the model's volumetric drag coefficient, $C_{DVmodel} \cong 7.5 C_F \cong 0.018$, is about 5% less than predicted by Eq. (2). At much lower Reynolds number, the use of Eq. (3) overestimates in some other cases, probably because laminar boundary layers persisted over significant portions of the models tested. The only large discrepancy is for a smooth sphere in the transcritical regime,[12] when the reported value of $C_{DVmodel}$ is about double that predicted. Hence, Eq. (2) must be treated with caution as $\lambda \rightarrow 1$.

Table 1   Comparison of model volumetric drag coefficients using data from various sources[2−12]

Model	λ	L, m	V, m³	$Re/10^6$ model	$C_{DVmodel}$	C_{DVH}[a]	$C_{DVmodel}/C_{DVH}$
R26[2]	10.15	1.22	0.0123	2.0	0.037	0.036	1.0
R32[3]	9.37	1.4	0.0193	1.7	0.028	0.036	0.78
Shenandoah[4]	8.6	1.72	0.0349	2.5	0.031	0.033	0.95
R33[5]	8.33	1.22	0.0139	2.1	0.024	0.034	0.7
Ellipsoid with trip[6]	8	0.15	3×10^{-5}	1	0.033	0.039	0.85
R101[7]	5.57	1.24	0.0289	49	0.018	0.019	0.95
SSZ[8]	4.75	0.87	0.015	0.7	0.029	0.039	0.76
ZMC-2 form[9]	3	1.76	0.301	2.1	0.026	0.034	0.74
Ellipsoid[10,11]	1.8	0.36	0.0237	0.6	0.065	0.064	1.0
Smooth sphere[12]	1	0.175	0.0028	6	0.23	0.11	2.1

[a]Equation (2).
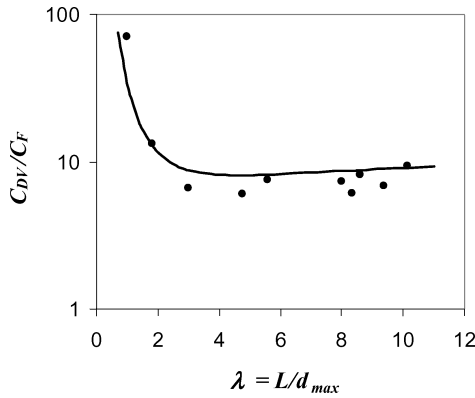
Fig. 1   Volumetric drag coefficient of axisymmetric bodies (Table 1) vs fineness ratio, compared with Eq. (2).

A plot of Eq. (2), as well as the drag coefficient data from Table 1, is shown in Fig. 1. Figure 1 shows that minimum drag (about $8C_F$) occurs when $\lambda = \lambda_{min} \cong 4.65$ in accordance with the prevailing design notion, but the curve near this minimum is surprisingly flat. A relatively small drag rise results from the adoption of lower values of λ down to about 2, for example, about 10% rise when $\lambda = 2.8$, and an even smaller drag rise is incurred by higher values of λ up to about 8.

Note that λ_{min} is independent of Reynolds number and Eq. (2) does not include any other shape parameters, for example, the station at which the maximum diameter occurs. This suggests that C_{DV} is insensitive to body contour shape. The ill-defined proviso that the body is streamlined appears to be sufficient for the reasonably good application of Eq. (2) at high Reynolds number when the boundary layer over most of the body surface is turbulent. This view is supported by previous computational studies[13,14] that used an evolution strategy to determine the body contour for minimum C_{DV}. When started with an ellipsoid body with $\lambda = 2.3$ and $C_{DV} = 0.0157$, successive shape mutations at $Re = 100 \times 10^6$ were found to evolve a more slender body with $\lambda = 4.26$ and $C_{DV} = 0.0143 \cong 0.9C_{DVH}$, that is, detailed numerical optimization only resulted in a drag reduction of about 9%. At much lower Reynolds number, when there is a potential to maintain significant areas of laminar boundary layer, body shape admittedly becomes more important: Larger drag reductions appear to be feasible by adopting shapes with a relatively long-slender forebody to maintain a favorable pressure gradient and thereby delay transition for a long as possible.[13−15]

When Fig. 1 is examined, aside from the flatness of the curve when $2 < \lambda < 8$, the other striking feature is the marked increase in drag when λ falls below about 2. This drag rise is caused by a growth in the aft-body separation region, that is, a rapid rise in pressure drag[10] (or form drag) as the streamlined body effectively becomes bluff. Given the apparent crudity of Eq. (2) at low λ, at first sight it would seem wise for the airship designer to avoid this drag rise by a significant margin and only consider designs with $\lambda > 2$. On the other hand, in some lighter-than-air vehicle design cases

(in particular, for pressurized, nonrigid types) there may be a strong desire for low λ, for example, to reduce the area and mass of the outer hull/envelope for a given gas volume. If there are no other design constraints, then it follows that the intermediate range $2 < \lambda < \lambda_{min}$ ought to be attractive. This appears to have been recognized by some airship designers. For example, Upson[16] adopted $\lambda = 2.83$ for the Metalclad ZMC-2 airship built in 1929, a value that was relatively low compared to other airships at that time.[17,18] When Eq. (3) is used, at $Re \cong 94 \times 10^6$ based on the length of the ZMC-2 hull, at a maximum airspeed of 27.7 m/s, $C_F \cong 0.0026$ and Eq. (2) give $C_{DVH} \cong 0.019$.

Drag Coefficients of Airships in Cruise

In practice, the total drag of full-scale airships in steady flight is considerably larger than the values predicted by Eq. (2) because of parasitic and interference drag terms caused by the addition of various appendages to the bare hull. The total volumetric drag coefficient C_{DVtot} of the whole/complete airship (including gondola, rigging, empennage, etc.) can be found by inverting the following equation:

$$P_{tot} = DU_{max}\big/\eta_p = \tfrac{1}{2}\rho U_{max}^3 C_{DVtot}V^{\frac{2}{3}}\big/\eta_p \qquad (4)$$

where P_{tot} is the total engine power output and η_p is the overall propulsive efficiency. Table 2 lists some estimates of C_{DVtot} found using Eq. (4) and data from various sources[4,5,18−23] assuming (for convenience) that $\eta_p = 65\%$ and $\rho = 1.2$ kg/m³ in all cases at the maximum quoted flight velocities. For example, using specifications[7,18] for the R101 the total drag coefficient C_{DVtot} is estimated to be about 0.025 at $Re = 465 \times 10^6$, which is about 40% higher than the value of $C_{DVmodel}$ at $Re = 49 \times 10^6$ given in Table 1. Note that using Eq. (2) the predicted volumetric drag coefficient of the R101 bare hull should be about 0.014 at $Re = 465 \times 10^6$; hence, C_{DVtot} is almost double the predicted bare hull value at the same flight Reynolds number. When similar data for other airships listed in Table 2 are examined, this rule-of-thumb appears to be typical. When $C_{DVtot} = NC_{DVH}$, in the range $2.83 < \lambda < 10.18$, N is found to be 2.3 ± 0.7, and it is not unreasonable to assume that this factor is, to first order, independent of Reynolds number.

Before proceeding, it is worthwhile checking this rule-of-thumb concerning the factor N using an alterative approach because the assumption that $\eta_p = 65\%$ and $\rho = 1.2$ kg/m³ in all cases is questionable, that is, the airships listed in Table 2 may have had different cruise altitudes and varying propeller efficiencies.

Drag Coefficients of Decelerating Airships

In principle, during periods of coasting (zero thrust), it is also possible to deduce the steady drag coefficient of any airship assuming straight and level flight in a near-neutral buoyancy condition. The equation of rectilinear motion is given by[24]

$$\rho V \frac{dU}{dt} + \rho V k_x \frac{dU}{dt} = -\frac{1}{2}\rho U^2 C_{DVtot}V^{\frac{2}{3}} \qquad (5)$$

Table 2   Estimates of drag coefficients using Eq. (4) and data from various sources[4,5,18−22]

Airship	λ	V, m^3	P_{tot}, kW	U_{max}, m/s	$Re/10^6$ maximum	C_{DVtot}[a]	C_{DVH}[b]	$C_{\text{DVtot}}/C_{\text{DVH}}$
R29[19]	10.18	30,016	615	24.1	263	0.049	0.017	2.9
R26[20]	10.15	29,860	764	26?	253	0.049	0.017	2.9
Shenandoah[4,17,18]	8.64	60,363	1,342	28	367	0.043	0.016	2.7
R33[5]	8.33	61,872	932	26.8	350	0.034	0.016	2.1
Zeppelin L43[17]	8.23	60,598	624	24.8	325	0.029	0.016	1.8
Los Angeles[18,21]	7.23	80,420	1,469	32.7	436	0.024	0.015	1.6
R101[7,18]	5.57	168,447	2,181	31.3	465	0.025	0.014	1.8
SSE3 100,000[22]	4.6	3,143	149	25	85	0.048	0.018	2.7
Skyship 600[23]	3.88	6,666	380	28.3	111	0.051	0.017	3.0
ZMC-2[17,18]	2.83	5,726	328	27.7	94	0.05	0.019	2.7
SPAS-13[23]	1	1,167	75	13.3	12	0.31	0.10	3.1
SPAS-70[23]	1	2,605	298	18.0	20	0.29	0.09	3.2

[a]Equation (4).   [b]Equation (2).

Table 3   Effective drag coefficients from previous deceleration tests[5,19−22,25−27]

Airship	λ	L, m	V, m^3	$Re/10^6$ test	C_{decel}[a]	C_{DVH}[b]	$C_{\text{decel}}/C_{\text{DVH}}$
R29[19]	10.18	164	30,016	220–60	0.045	0.017–0.02	2.6–2.2
R26[20]	10.15	163	29,860	180–90	0.049	0.018–0.02	2.7–2.5
R32[25]	9.37	187	46,156	380–95	0.037	0.016–0.019	2.3–1.9
R33[5]	8.33	196	61,872	305–130	0.035	0.016–0.018	2.2–1.9
Zeppelin L43[26]	8.23	197	60,598	300–90	0.032	0.016–0.018	2.0–1.8
Los Angeles[21,27]	7.23	200	78,155	400–185	0.027	0.015–0.017	1.8–1.6
SSZ[22]	4.7	45	2,010	60–20	0.036	0.019–0.022	1.9–1.6
SSE3 100,000[22]	4.6	51	3,143	70–25	0.049	0.018–0.021	2.7–2.3
TE-2[27]	4.0	41	2,271	45–30	0.045	0.019–0.021	2.4–2.1
Puritan[27]	3.5	39	2,432	55–20	0.046	0.019–0.022	2.4–2.1
ZMC-2[27]	2.83	46	5,726	90–30	0.043	0.019–0.023	2.3–1.9

[a]Equation (7).   [b]Equation (2).

where k_x, the inertia coefficient, accounts for the added mass (also known as virtual or apparent mass) effect brought about by energy changes in the flowfield.[10] For potential (frictionless) flow, this coefficient is a constant for any given hull geometry, and it can be calculated exactly, but for viscous flows with separation, it cannot be easily determined. In practice, the accurate deduction of the separate terms C_{DVtot} and k_x from deceleration data is problematic. Previous studies[19,22,25] have consequently rewritten Eq. (5) in a more convenient form,

$$\rho V \frac{dU}{dt} = -\frac{1}{2}\rho U^2 C_{\text{decel}} V^{\frac{2}{3}} \tag{6}$$

where C_{decel} is the effective nonsteady drag coefficient. If this term is assumed to be constant, then its value can be determined from flight data by plotting a graph of $1/U$ vs t over a short time period and measuring the gradient $d(1/U)/dt$ because

$$C_{\text{decel}} = -2V^{\frac{1}{3}}U^{-2}\frac{dU}{dt} = 2V^{\frac{1}{3}}\frac{d(1/U)}{dt} \tag{7}$$

Table 3 lists the results of previous airship deceleration tests[5,19−22,25−27] using Eq. (7). It can be seen that the values of C_{decel} deduced are up to 21% lower than the respective values of C_{DVtot} calculated for the same airships using Eq. (4) in Table 2. This is roughly consistent with the expectation that $C_{\text{decel}} = C_{\text{DVtot}}/(1+k_x)$ for potential flows.[24] Hence, the finding that $N \cong 2.3 \pm 0.7$ in the range $2.83 < \lambda < 10.18$ is independently substantiated. The only discrepancies to this rule-of-thumb are the two airships listed at the bottom of Table 2, which are discussed in the next section.

Spherical Airships

Recently a Canadian company[23] has set an interesting design precedent by developing a series of near-spherical airships (or perhaps more accurately dirigible balloons) with $\lambda \cong 1$. Aside from

reduction in hull mass brought about by adopting the lowest feasible surface-area-to-volume ratio, the added advantage of adopting a near-spherical form is that no empennage is required because there is neither destabilizing yaw nor pitch moments. There may also be some secondary gains, for example, rapid yaw maneuvers ought to be achievable with relatively little power. On the other hand, whereas the use of Eq. (2) is doubtful as $\lambda \to 1$, there is little doubt that the drag of a near-spherical airships will be considerably larger than the drag of streamlined airships with the same V and Reynolds number.

Drag Coefficients of Spheres and Spherical Airships

There is plenty of wind-tunnel data in the literature on the drag of smooth spheres for Reynolds number below about 1 million, but hardly any data above. When the results of Achenbach[12] are used, the drag coefficient of rear-mounted spheres tends to about 0.24 as $Re \to 6 \times 10^6$ in the transcritical regime. Note, however, that such experiments are difficult to repeat accurately. Drag measurements on spheres are highly sensitive to factors such as surface smoothness and the tunnel turbulence levels. Most drag and pressure distribution measurements to date have also effectively been time averaged. The actual drag force on a sphere will fluctuate significantly because vortices are shed at frequencies of the order of U/d_{max}. Intermittent lift-induced drag resulting from this shedding is probably quite sensitive to any flow asymmetries. Nevertheless, despite these reservations, it is interesting to compare the cited experimental value with available flight data on the Canadian near-spherical airships.[23]

When the quoted figures for maximum flight velocity are accepted and assumed values of $\eta_p = 65\%$ and $\rho = 1.2$ kg/m^3 (again, for uniformity in Table 2) are used, Eq. (4) predicts that the two airships SPAS-13 and SPAS-70 would have $C_{\text{DVtot}} \cong 0.29$–0.31 in the range $20 \times 10^6 > Re > 12 \times 10^6$. Hence, the full-scale airships appear to have drag coefficients that are about 20–30% higher than predicted by tunnel tests: a result which is not unreasonable.

Of course, these drag coefficient values are much larger than the estimates for the other streamlined bodies and airships listed in Tables 1 and 2, suggesting (at first sight) that there must be a large propulsive benefit in shifting, for example, to $\lambda > 2$.

Possible Advantage of Low Fineness Ratio

Because $dC_{DV}/d\lambda$ is negative when $\lambda < \lambda_{min}$, propulsion system mass should increase as λ is lowered. The question that arises is whether or not this increase offsets any reduction in hull mass resulting from decreases in surface-area-to-volume ratio, as well as possible reductions in empennage mass while maintaining pitch and yaw stability.

To carry out a first-order tradeoff study (with λ as a continuous variable), it can be assumed that V is fixed while the propulsion system, empennage, and hull masses vary. If it also assumed that the power-to-mass ratio of the propulsion system is a constant, p_m, and a fixed cruise velocity U has to be achieved, then the propulsion system mass $M_{prop} = P_{tot}/p_m$ will increase in proportion to C_{DVtot} according to Eq. (4). Empennage mass M_{emp} is difficult to estimate, because it depends on what assumptions are made about maneuvers and how relaxed the control system is allowed to be. Hull mass M_{hull} is also difficult to estimate because it depends on the structural layout and loading conditions, for example, the bending moment acting on the hull.[17] The simplest assumption that can be made (if only to gain some first-order insight) is that both these masses are linear functions of λ,

$$M_{emp} + M_{hull} = a + b\lambda \qquad (8)$$

where a and b are constants whose values are uncertain. If it is further assumed that the there is an overriding need to optimize the disposable load, then it follows there is a need to minimize $M_{sum} = M_{prop} + M_{emp} + M_{hull}$. Combining Eq. (4) and Eq. (8) and differentiating with respect to λ yields

$$\frac{dM_{sum}}{d\lambda} = \left(\frac{1}{2}\rho U^3 S_{ref}\eta_p^{-1} p_m^{-1}\right)\frac{dC_{DVtot}}{d\lambda} + b \qquad (9)$$

Hence, it is beneficial to increase λ (below λ_{min}) when

$$\left|\frac{dC_{DVtot}}{d\lambda}\right| > 2bp_m\frac{\eta_p}{(\rho U^3 S_{ref})} = \left(\frac{C_{DVtot}}{\lambda}\right)\frac{(M_{emp} + M_{hull} - a)}{M_{prop}} \qquad (10)$$

At this stage, it would be prudent to have a more complete data set on the drag of spheroids/ellipsoids (etc.) for $1 < \lambda < 2.8$ at (or close to) the relevant Reynolds number range to estimate $|dC_{DVtot}/d\lambda|$. Unfortunately, relevant empirical data appears to be scant, much poorer than the data set for spheres. To proceed, it is necessary to resort to Hoerner's formula again despite that it is no longer accurate when $\lambda = 1$. Differentiating Eq. (2) with respect to λ yields

$$\frac{dC_{DVH}}{d\lambda} = C_F\left(\frac{4}{3}\lambda^{-2/3} - 7\lambda^{-13/6} - 64\lambda^{-11/3}\right) \qquad (11)$$

When $\lambda = 1$, $|dC_{DVH}/d\lambda| \cong 70C_F \cong 2C_{DVH}$. Furthermore, if it assumed that $C_{DVtot} = NC_{DVH}$ and N is roughly constant, then at $\lambda = 1$, it is not unreasonable to expect that $|dC_{DVtot}/d\lambda| \cong 2C_{DVtot}$.

When Eq. (10) is used, it follows that if the propulsion system mass of a near-spherical airship is greater than about half the combined hull and empennage masses then it would certainly be beneficial to increase λ. However, if the propulsion system mass is much smaller, that is, when low cruise velocity targets are set, then the advantage of increasing λ is not certain. More simply, spherical airships may be justified when the target cruise velocity (or dynamic pressure in cruise) is deliberately set below some upper limit implied by Eq. (10).

Note that no allowance has been made for any fuel mass because this term is assumed to be included with the disposable mass. If an extended analysis had been presented here, then it could also have been shown that there is some limiting range or endurance target below which increases in λ are not justified. Finally, note
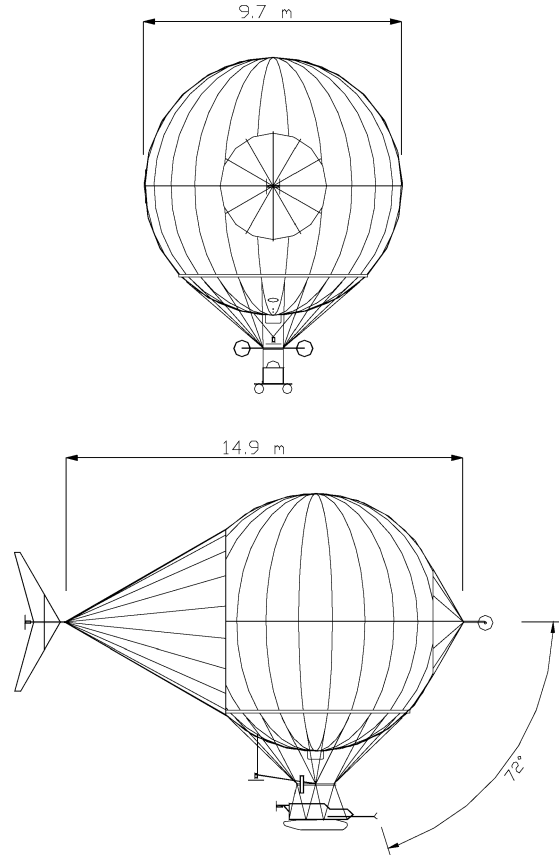

Fig. 2 Front and side views of spheroid-cone airship "White Diamond."

that disposable mass is not necessarily the overriding optimization parameter. Indeed, it is likely that costs and operating logistics will be principal concerns. The essential point to make is that low λ airships cannot be dismissed easily. In some cases, low λ, or even $\lambda = 1$, may offer an optimum design solution to meet certain specific mission requirements within certain cost constraints, albeit at some risk.

Airship with a Spheroid-Cone Form

With the preceding background in mind, in 2002 the author instigated the development of a new airship for an on-going project concerned with scientific exploration of rainforest canopy.[28,29] In essence the airship had to lift two people (including the pilot) and be capable of stable yet maneuverable flight in quiescent (still air) tropical conditions, effectively replacing an older design tested by the author.[29,30] Because the required maximum flight speed target was unusually low, just 3 m/s, it followed that an airship with low λ, or even $\lambda = 1$, might provide the best design solution. Indeed, it was finally decided to adopt a spheroid-cone hull form with $\lambda = 1.54$ (Fig. 2). To reduce risk, this major design decision was preceded by a brief evaluation study using several wind-tunnel models.

Wind-Tunnel Measurements of Drag

Two closed-circuit wind tunnels at the author's present address were used for testing: tunnel 1 with a contraction of 7.2:1 and a quasi-octagonal working section 1.24 by 1.0 m and tunnel 2 with a contraction of 5.6:1 and a rectangular working section 1.0 by 0.77 m. The turbulence levels of both tunnels were estimated (using hot-wire techniques) to be less than 0.4% at the test flow speeds involved, about 35–43 m/s. Because no suitable rear-mounting sting was available at the time, the models were side mounted on a simple, vertically hanging, pendulum balance. The resulting force on the balance was measured with a resolution of 0.1 N. The models were attached to a streamlined strut with a chord of 18 mm and thickness of 6 mm. The tare drag of this strut was measured separately

Table 4   Summary of wind tunnel tests

Model	λ	V, m^3	$Re/10^6$ model	C_{DVmodel}	C_{DVH}[a]	$C_{\text{DVmodel}}/C_{\text{DVH}}$
Spheroid-cone with trip	1.47	0.00086	0.35	0.12	0.093	1.3
Spheroid with trip	1.07	0.00086	0.35	0.26	0.16	1.6
Wooden sphere	1	0.00163	0.35	0.32	0.18	1.8

[a]Equation (2).
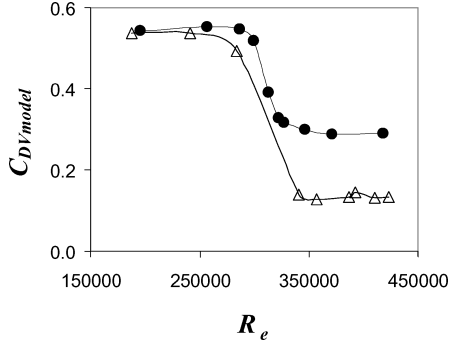
Fig. 3   Volumetric drag coefficients of sphere and spheroid-cone (triangle symbol), vs Reynolds number.

and subtracted from the combined model plus strut drag results. No allowance was made for mutual interference, but because the study was intended as a preliminary comparative evaluation, this methodology was deemed acceptable. To begin, several prolate ellipsoids of various sizes (ranging from about 120 to 600 mm in length) were tested with $\lambda = 1.35$, 2.0, and 4.0. The results of these tests do not warrant inclusion here. It is sufficient to state that, although they largely supported the trends predicted by Hoerner's formula, Eq. (2), the drag coefficients were found to be 15–30% higher (in both tunnels) probably because of the strut interference and/or blockage effects in one case.

After these preliminary tests, a varnished wooden sphere 146 mm in diameter and an aluminium spheroid form with $\lambda = 1.07$, and 122 mm in diameter, were both investigated with and without a series of plastic cones with semi-apex angles of 0.52 rad attached to their rear surfaces. With the rougher wooden sphere, transition occurred when $Re \cong 3 \times 10^5$. However, with the smoother aluminium spheroid, transition had to be forced using a trip wire (about 0.07 mm in diameter) placed on the upstream side, about 1.4 rad from the body center and major axis. Consequently, in all tests, a cone was placed (symmetrically, at zero incidence) within a supercritical separated wake. Without cones added, the volumetric drag coefficients of the sphere and spheroid were found to be about $C_{\text{DVmodel}} = 0.26$–0.32, at about $Re \cong 4 \times 10^5$ (Table 4). Once again, this drag coefficient was higher than expected probably because of strut interference. Also, no allowance was made for blockage effects. Addition of each cone was found to decrease C_{DVmodel} markedly, and tuft wand tests indicated there was an associated reduction in wake diameter. This suggests the cones did not prevent separation, but did reduce the size of the separated wake and, hence, reduced pressure drag. The lowest value of about $C_{\text{DVmodel}} = 0.12$ (based on the same spherical volume) was obtained with the largest cone, which had a base diameter of 100 mm, at $Re \cong 3.5 \times 10^5$ (Fig. 3). This drag result is about 30% higher than predicted by Eq. (2), but the value of $|dC_{\text{DVmodel}}/d\lambda|$ implied by these tests was also about 30% higher than predicted by Eq. (11). Note also that placing the largest cone at incidence to the flow resulted in only minor increase in drag: about 10% increase at 0.2 rad.

At the end of the evaluation study it was, therefore, sensible to assume that, provided similarly favorable flow effects exist at the much higher Reynolds number expected for the full-scale airship, an overall performance gain would be possible by the attachment of a rear-facing cone to a spherical balloon, reducing C_{DVtot} and, hence, reducing the mass (and cost) of a propulsion system.

Description of Flight Tests of Full-Scale Airship

Following the wind-tunnel evaluation study, a decision was made to commit to the full-size airship design shown in Fig. 2. This spheroid-cone airship was tested using tethers inside shed 1 at Cardington, United Kingdom (in January 2004), and then flown freely over the Kaieteur National Park, Guyana (in July 2004). The main balloon had a diameter $d_{\max} = 9.7 \pm 0.05$ m and, hence, was capable of containing $V_{\text{He}} = 480 \pm 5$ m^3 of helium when filled at its maximum allowable internal pressure. The tail cone was made of a light fabric and had a length of about 6 m with a semi-apex angle of 0.52 rad. The cone was held in tension by an internal alloy tube running along the central longitudinal axis, and tightly attached to the balloon in 24 places on a pitch circle diameter of 7 m. It was not sealed and filled with nonpressurized air with an internal volume of about $V_{\text{cone}} = 43$ m^3. A small nose cone of about 1.5 m^3 (also air filled) was also fitted around a bow pole on the central longitudinal axis. Consequently, the total hull volume was $V = 524.5 \pm 5$ m^3, the hull length was $L = 14.9$ m, and the fineness ratio was $\lambda \cong 1.54$.

The airship was flown by the author over Kaieteur at about 450–490 m above sea level, when the ambient air temperature was $23.2 \pm 1°$C at 95% humidity. The local wind speed during the flight tests was less than 2 m/s measured in a large clearing at a height of about 10 m above ground level. The ambient density was estimated to be $\rho = 1.125 \pm 0.003$ kg/m^3, so that the total inertial mass (not including added mass) of the airship, $M_{\text{tot}} = (\rho - \rho_{\text{He}})V_{\text{He}} + \rho_{\text{He}}V_{\text{He}} + \rho V_{\text{cone}} = \rho V$, was about 587 ± 10 kg.

The propulsion system of the airship was made up of several electric motors, powered by a rechargeable lithium-ion battery with a mass of 40 kg, each driving propellers about 0.6 m in diameter. For forward thrust, two motors were mounted side-by-side of a hanging gondola, one was mounted directly behind the gondola, and one motor was mounted at the extreme aft position, axially on the alloy tube. The thrust F_i of each of these units had been previously measured in tunnel 1 at a similar temperature, but at higher density, $\rho_{\text{tunnel}} = 1.225$ kg/m^3, and simple linear equations were used to predict their thrust in ambient conditions,

$$F_i = \varphi_i F_{Si}(1 - U/u_F)\rho/\rho_{\text{tunnel}} \qquad (12)$$

where $\varphi_i(t)$ is the throttle setting, F_{Si} is the static thrust, and u_F is a thrust decay rate constant found from testing the motors at a fixed voltage. No allowance was made for negative blockage effects in the tunnel. During flight, the throttle setting of each motor φ_i was assumed to ramp up and down linearly between 0 and 1 within 5 s, and an audio recording was made to determine which motor was being operated at any particular time.

Adequate yaw stability was achieved by the addition of a fixed vertical fin of about 4 m^2. Control in yaw was achieved by either slewing the aft motor or using a bow thruster assembly: two electric motors driving 0.56-m-diam propellers in the lateral direction mounted on the front of the bow pole. Vertical height control was achieved by either venting helium, dropping ballast, pitching the side mounted motors, or using a vertically mounted motor driving a 0.71-m-diam propeller.

Flight speed was measured using a three-axis Metek USA-1 Basic sonic anemometer with a data acquisition rate of 10 Hz. In tunnel 1, this anemometer produced a fairly uniform white noise error at 10 Hz, with a root-mean-square velocity fluctuation of about $u_{\text{rms}} = 0.05$ m/s, at flow speeds between 1 and 3 m/s. The anemometer was mounted on a sting in front of the gondola at a radial distance of about $r = 6.6$ m from the balloon's center at about $\theta = 1.26$ rad from the major axis (Fig. 2). A (fixed) flow speed correction factor

of 0.88 was calculated to estimate the forward flight speed, $U = U_\infty$, from the measured (higher) value, U_θ, at the sting position using the potential flow equation for flow around a sphere[31]

$$U_\theta = -\tfrac{1}{2}U_\infty \sin\theta \left[2 + \left(\tfrac{1}{2}d_{max}/r\right)^3\right] \quad (13)$$

No account was taken for effective variations in anemometer position θ brought about by yaw and pitch changes.

Drag in Cruise

To find the steady value of C_{DVtot}, the spheroid-cone airship was flown with one motor running (with $\varphi_i = 1$) in a near-neutral buoyancy state so that the flight trajectory was approximately straight and level with minimal control input. The drag coefficient was estimated assuming $F_i = D$ in Eq. (1). When the aft motor was used for a duration of about 120 s, a near-steady value of about $U = 1.1$ m/s (averaged over 5 s and corresponding to $Re \cong 1 \times 10^6$) was reached. The steady drag coefficient was, hence, found to be $C_{DVtot} \cong 0.34 \pm 0.6$. This error margin accounts for all of the variations in the parameters used in Eq. (1), but does not include the experimental and theoretical uncertainties involved in the estimate of F_i. It is also subject to a standard deviation of about 0.09, resulting from fluctuations in the velocity data, which include the anemometer's intrinsic noise. Again, note that the actual drag of the spheroid-cone airship probably does fluctuate significantly as vortices are shed intermittently in the aft-body separation region, and so this deviation does not necessarily represent experimental error.

Deceleration Tests

A deceleration graph for the spheroid-cone airship is shown in Fig. 4. When a least mean squares method was used, the gradient $d(1/U)/dt$ of the linear regression line through these data is about 0.02 m^{-1} over a period of about 20 s with a fit of $R^2 = 0.7$, and Eq. (7) gives $C_{decel} = 0.32 \pm 0.03$; however, the scatter in the data is large. A second deceleration graph covering a slightly lower velocity range is shown in Fig. 5. The gradient is increased to about 0.03 m^{-1} over a period of about 27 s with a fit of $R^2 = 0.59$, giving $C_{decel} = 0.47 \pm 0.04$, but the scatter is still larger and the linear fit is poorer. In the latter test, a slightly better fit with Eq. (6) was found when $C_{decel} \cong 0.3/U$ for flight velocities between about 1.1 and 0.4 m/s, corresponding to the range $1 \times 10^6 < Re < 3.6 \times 10^5$.

Reconstruction of Flight Model

With the drag coefficient estimates deduced, a predictive model of $U(t)$ was constructed by numerically integrating the following equation of motion assuming $k_x = 0.2$ and $C_{DVtot} = 0.32$ for $U > 1.1$ m/s and $0.36/U$ for $U < 1.1$ m/s:

$$\rho V (1 + k_x) \frac{dU}{dt} = \Sigma F_i - \frac{1}{2}\rho U^2 C_{DVtot} V^{\frac{2}{3}} \quad (14)$$
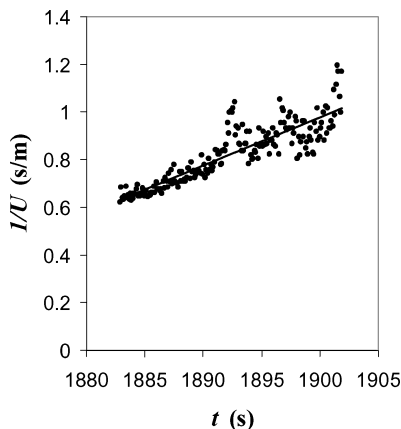
Fig. 4 Reciprocal of forward flight velocity vs flight time during phase of deceleration (with zero thrust).
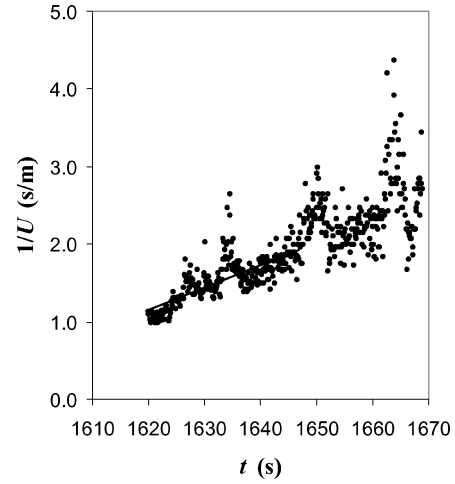
Fig. 5 Reciprocal of forward flight velocity vs flight time during phase of deceleration (with zero thrust).
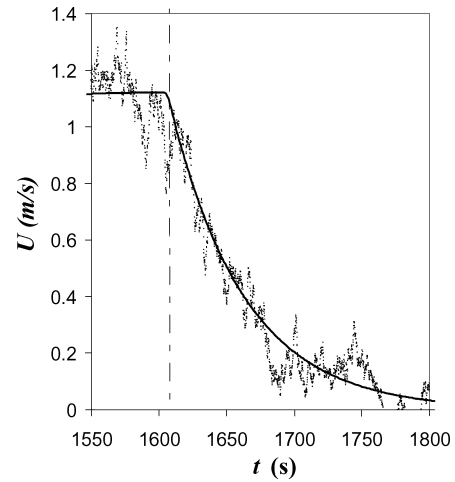
Fig. 6 Forward flight velocity vs time: ——, dynamic model prediction.

A sample trace of the recorded data is shown in Fig. 6, together with the dynamic prediction. For the corresponding thrust history with the aft motor used alone, $F_{Si} = 18$ N and $u_F = 15$ m/s. In this data sample, note that there is a constant thrust phase from 1500 to 1610 s and a zero-thrust deceleration phase from 1610 to 1800 s. There appears to be good agreement between most of the data and the prediction, although this success is deceptive because C_{DVtot} has effectively been found by fitting the data in the deceleration phase. The value of $k_x = 0.2$ was chosen because it is consistent with $C_{decel} = C_{DVtot}/(1 + k_x)$ and the finding that $C_{decel} \cong 0.3/U$ for $U < 1.1$ m/s. However, note that a reasonable looking fit appears to be possible for quite wide variations ($\pm 20\%$) in C_{DVtot} and C_{decel}, and it is not possible to determine the value of k_x with any confidence. An estimate of the errors and a rigorous statistical analysis to find the best parameter fit is not presented here. One problem with such an analysis is that the total data set was limited to just one flight of about 2700 s recorded duration. Further flight testing would obviously be needed to establish statistical variations and repeatability.

During the test periods (described earlier) pitch and yaw variations were less than about ± 0.2 rad. The only exception is during the time period where the dynamic prediction appears to be poorest, from 1680 to 1800 s, when the airship velocity fell below 0.3 m/s corresponding to $Re < 3 \times 10^5$. At these low velocities, pitch and yaw changes were much larger, and then Eq. (14) is clearly inadequate. During the decelerations shown earlier, note that the bow thruster was used to hold the airship's heading on a visual horizon reference point, but this was limited to a few short bursts of a

few seconds duration only. The other motors on the airship were not used during these test periods, and there was no helium/ballast release.

Discussion of Flight-Test Results

Comments on Drag Coefficient Estimate

From the flight tests, the cruise drag coefficient of the spheroid-cone airship was found to be $C_{DVtot} \cong 0.34 \pm 0.06$ at $U = 1.1$ m/s, $Re \cong 1 \times 10^6$. This value was higher than expected: With use of Eq. (2), it follows that $C_{DVH} \cong 16 C_F \cong 0.07$ and, hence, $N \cong 4.8 \pm 0.9$. However, this is not an unreasonable result because C_{DVtot} is also about three times higher than drag coefficient value of the bare spheroid-cone model measured during the wind-tunnel tests (Table 4 and Fig. 3). When the inaccuracy of Hoerner's formula [Eq. (2)] when $\lambda \to 1$ is considered, the result is not widely inconsistent with the other data in Table 2.

This relatively high drag coefficient can probably be best explained by interference effects causing premature separation. It cannot be fully accounted for by separate parasitic terms acting alone: the drag of the rigging supporting the gondola, the drag of the tail fin, and the drag of the gondola itself. When the estimation methods presented by Hoerner[1] are used, these parasitic terms probably only accounted for about 10–20% of the total drag. However, because of interference with the hull, their combined effect was probably considerably larger. Some experimental evidence[9] suggests that interference effects of any hull protuberances will be more pronounced on hull forms with low λ. In particular, note that at the base of the balloon there was a cylindrical fabric protrusion (about 0.6 m in diameter, 0.4 m depth) caused by one of the helium relief valves (Fig. 2). Based on previous experiments,[9] it is likely that this valve unit alone caused a significant drag rise. Another possibility is that the rigging lines tended to produce scalloping in the lower balloon envelope and that may have also caused flow separation upstream of the maximum diameter. Flutter in the fabric tail cone and fin might have also brought about adverse flow effects. (Both surfaces were stretched taut, but flutter was observed while the airship was being held on the ground during sporadic breezes exceeding 2 m/s.)

Another possible reason for the high drag coefficient (which would be of more general aeronautical interest, but is difficult to quantify with present knowledge) is some kind of detrimental, wake-amplifying interaction with atmospheric eddies or microgusts with wavelengths comparable with the airship's length.[32] About 20 m above the forest canopy, the drift velocity of the airship was about 1 m/s between the aforementioned tests, and so an atmospheric boundary layer with associated turbulence would have been present. This atmospheric turbulence should not be confused with the much smaller-scale turbulence in the boundary layer over the envelope. Whereas energy input into a turbulent boundary layer can often be stabilizing, changes in local flow incidence caused by the impingement of much larger-scale atmospheric eddies on the hull are more likely to have caused locally premature flow separation. Fourier analysis of different blocks of flight velocity data was carried out to find the power density spectrum. In all cases, the dominant frequencies were found to occur at or below 0.1 Hz, although there was also a pronounced spike at around 0.2 Hz. This spike can be explained by the gondola (and anemometer sting) oscillating in pitch during flight about 0.05 rad, effectively like a pendulum with a length of 6 m. The lower frequency noise, however, can be best explained by turbulent eddies in the atmospheric boundary layer with wavelengths greater than about 5 m. The root-mean-square velocity fluctuation was typically $u_{rms} \cong 0.08$ m/s, somewhat greater the aforementioned noise of the anemometer.

Aside from the relatively high drag coefficient value, at a mean flight speed of 1.1 m/s there does not seem to be a large difference between the deduced values of C_{DVtot} and C_{decel}. This suggests that added mass effects were not as large as might be anticipated for a low λ hull. (For example, for a sphere in a potential flow,[33] $k_x = 0.5$, and so a difference of up to about 50% in C_{DVtot} and C_{decel} might be expected.) However, before discussing nonsteady flow effects further, note that the flows induced by the thrust units themselves may have substantially altered the flow around the airship, thereby altering its drag. In particular, it is likely that the flow induced by the aft propeller modified the separation region presumed to have surrounded the cone. Tufts were added to the cone, but as indicators of separation they were not conclusive.

The beneficial effects of placing a propeller at the aft of an airship hull model have been reported by McLemore.[34] The most favorable (but probably unrealistic) design assumption is that an aft-mounted propeller could actually prevent or alleviate the aft-body separation and, thereby, reduce hull drag significantly. Alternatively, an aft propeller could induce higher flow velocities near the apex of the cone, resulting in a reduction in pressure and increased drag.[35,36] Hence, the use of the aft motor (alone) on the spheroid-cone airship might have effectively decreased or increased the cruise drag coefficient. To determine whether either effect was significant, it would be necessary to repeat the cruise drag test using the alternative motors to provide steady thrust.

Additional Comments Concerning Nonsteady Flow Effects

There are fundamental grounds to expect that the drag of a decelerating/accelerating bluff body will differ markedly from the steady value even after allowing for added mass effects using potential flow estimates for k_x. Previous studies[37–39] have shown that k_x is strongly dependent on the instantaneous acceleration/deceleration modulus, $A = L|dU/dt|/U^2$ and possibly Reynolds number. There is also some evidence that the effective drag force measured at any one instant is also dependent on the acceleration history preceding that instant.[40,41]

The faster deceleration test shown in Fig. 4 was preceded by a phase of acceleration, but there was insufficient evidence in the entire data set to determine whether this history was relevant. When it is assumed C_{decel} was constant during this deceleration phase, $A \cong 0.3$. The velocity and distance flown by the airship after some time t after the commencement of deceleration can be estimated by integrating Eq. (6),

$$U = U_0/(1 + U_0 t/L_{decel}) \qquad (15)$$

$$s = L_{decel} \, \ell n (1 + U_0 t/L_{decel}) \qquad (16)$$

where U_0 is the initial velocity (in this case about 1.6 m/s) and $L_{decel} = 2V^{1/3}/C_{decel} \cong 50$ m. After about 30 s, when $U_0 t/L_{decel} \cong 1$, the airship's velocity would have been halved and the distance flown would have been $s \cong 35$ m, or about $2.3L$. Similarly, during the slower deceleration test shown in Fig. 5, the deceleration modulus was larger and the distance involved would have been even shorter. Compared with previous deceleration tests[5,19–22,25–27] on other (much larger and faster) airships, both these decelerations were, therefore, relatively rapid and occurred over relatively short distances. This suggests that wake recontact[39,41] was a plausible interacting phenomena and that it may have had a significant influence on the velocity data recorded.

If an airship decelerates sufficiently rapidly, then the wake entrained behind the airship could effectively converge on the hull and possibly overtake it. Munk[26] investigated this possibility while analyzing deceleration data on Zeppelin rigid airships using a highly idealized wake model, but concluded wake recontact was implausible because the airships concerned decelerated far too slowly in forward flight. For the spheroid-cone airship, however, the same idealized model predicts wake recontact could have occurred during the deceleration tests carried out.

The effects of wake recontact are no doubt complex and can only be speculated on. Aside from an ambiguous influence on the airship's drag coefficient, it is possible that the local flow velocity at the position of the anemometer could have been reduced temporally,[26] that is, distinct fluctuations in the velocity data ought to be observed some time after deceleration starts. Indeed, when Figs. 4 and 5 are examined, candidate velocity fluctuations are conspicuous at various times after the start of both decelerations. Whereas these fluctuations can be explained by atmospheric eddies, they might also be explained by recontact with the separate wakes of the gondola and the balloon.

Note that previous deceleration tests[22,27] on smaller airships also appeared to have suffered from large fluctuations in velocity data. Other deceleration tests[19−21,25,26] also indicated markedly increased values of C_{decel} toward the end of the deceleration tests, about 2–3 times higher than the values listed in Table 3. Whereas it has been stated[24] that these early tests effectively suffered from data acquisition and testing mistakes, for example, elevator control inputs and idling propeller drag, Munk[26] argued that the increase in C_{decel} was caused by a fundamental aerodynamic effect manifested by a distinct discontinuity in the slope of the relevant deceleration graphs. As has already been stated, Munk[26] rejected wake recontact, but he did not offer an explicit physical alternative. One possibility is that at some critical condition the turbulent boundary layer over a decelerating hull becomes unstable and separates prematurely, thereby increasing the drag coefficient. Conversely, during accelerations, a stabilizing effect, delaying separation and reducing drag, should, therefore, occur. If these two opposite effects exist, then they would both tend to offset the dynamic effects of added mass.

Summary

The principle outcomes of this design-motivated study were as follows:

1) Hoerner's formula, Eq. (2), has been confirmed as a good first order approximation for the drag coefficients of streamlined axisymmetric model bodies over a wide range of fineness ratios.

2) The steady flight drag coefficients of a sample of complete airships were found to be a factor N times larger than Hoerner's formula predicts, where $N = 2.3 \pm 0.7$. (The generally accepted explanation for this drag factor is parasitic drag caused by appendages and their interference with the hull.)

3) The drag coefficients of smooth spheres in the transcritical regime were found to be higher than Hoerner's formula predicts, and first-order estimates of the drag coefficients of recently built, Canadian, spherical airships indicated that N exceeds 3, which is relatively high compared to most streamlined airships, as might be expected. (Note, however, from an overall design standpoint, it does not follow that low fineness ratio airships should be rejected. Indeed they may offer some gains in certain applications.)

4) Wind-tunnel tests showed that the addition of a conical body to the aft of a spherical body reduces the drag coefficient by about 50% (based on the same spherical volume) in the supercritical regime (Fig. 3). This reduction (not previously reported) probably occurs because addition of the cone results in a reduction in the size of the separated wake.

5) Flight tests on a new (not previously reported) 480 m³ helium-filled airship with a spheroid-cone form were carried out, but the anticipated reduction in drag coefficient was not found. Instead, the factor N was found to be 4.8 ± 0.9. One reason for this relatively high drag factor may have been severe parasitic interference and/or atmospheric turbulence causing premature flow separation.

From a design standpoint, the high drag coefficient of the spheroid-cone airship is disappointing, not only because the value deduced for C_{DVtot} was larger than hoped, but also because it does not provide any firm evidence that the addition of the cone did actually reduce the drag below that of a near-spherical balloon without a cone and empennage. To determine the magnitude of any such reduction, it would be necessary to retest the airship with the cone and empennage removed. Unfortunately this has not yet been possible within the project constraints.

Note that the fabric cone on the airship was air filled, and the value of C_{DVtot} quoted earlier for the spheroid-cone is based on the total hull volume V. If the cone had been completed sealed and helium filled, then a buoyancy increase of up to about 8% could have been brought about. On the other hand, when drag coefficients are compared on an equal buoyancy basis, note that the spheroid-cone airship did not have a ballonet fitted. The actual mass of the cone and empennage was about 8 kg, so that if both items were removed it could permit a 15% increase in propulsion system mass. For the same endurance and flight speed, this can be translated into a potential 15% increase in power, that is, a 15% allowable increase in C_{DVtot}.

Although these rather specific results may not have any general importance, some of the speculations of this study will hopefully provoke broader scientific interest. In particular, the effects of atmospheric turbulence and nonsteady flow effects[37−41] (such as wake recontact) may have wider relevance and be worthy of further investigation. To understand these effects further, it may be worthwhile to carry out some full-scale flow visualization experiments and/or to recommence tests on representative models.[37,38] Comparison with computational fluid dynamic simulations is also called for.

References

[1]Hoerner, S. F., *Fluid Dynamic Drag*, Hoerner Fluid Dynamics, Bakersfield, CA, 1965, Chaps. 1–6.

[2]Pannell, J. R., and Jones, R., "Experiments on a Model of an Airship of the 23 Class," Aeronautical Research Committee, R&M, No. 456, His Majesty's Stationary Office, London, April 1918.

[3]Jones, R., and Williams, D. H., "Experiments on a Model of Rigid Airship R.32 Together with a Comparison with the Results of Full Scale Turning Trials and Consideration of the Stability of the Ship," Aeronautical Research Committee, R&M, No. 779, His Majesty's Stationary Office, London, April 1921.

[4]Zahm, A. F., Smith, R. H., and Louden, F. A., "Air Forces, Moments and Damping on Model of Fleet Airship Shenandoah," NACA TR 215, Nov. 1925.

[5]Frazer, R. A., and Gadd, A. G., "The Prediction of the Resistance of Rigid Airship R.33," Aeronautical Research Committee, R&M, No. 827, His Majesty's Stationary Office, London, July 1922.

[6]Judd, M., Vlajinac, M., and Covert, E. E., "Sting-Free Drag Measurements on Ellipsoidal Cylinders at Transition Reynolds Numbers," *Journal of Fluid Mechanics*, Vol. 48, Pt. 2, 1971, pp. 353–364.

[7]Jones, R., Williams, D. H., and Brown, A. F., "Tests on Two Streamline Bodies in a Compressed Air Tunnel," Aeronautical Research Committee, R&M, No. 1710, His Majesty's Stationary Office, London, April 1936.

[8]Frazer, R. A., and Simmons, L. F. G., "Investigation of the Forces and Moments Upon a Complete Model Airship of Type S.S.Z. with an Analysis of the Effects of Full and Partial Rigging," Aeronautical Research Committee, R&M, No. 457, His Majesty's Stationary Office, London, July 1918.

[9]Ower, E., "Some Aspects of the Mutual Interference Between Parts of Aircraft," Aeronautical Research Committee, R&M, No. 1480, His Majesty's Stationary Office, London, June 1932.

[10]Duncan, W. J., Thom, A. S., and Young, A. D., *Mechanics of Fluids*, 2nd ed., 1970, pp. 151–155, 239–246.

[11]Prandtl, L., *Ergebnisse der Aerodynamischen Versuchsanstalt zu Göttingen*, Oldenbourg, Munich, 1925, Chap. 4, pp. 30–32.

[12]Achenbach, E., "Experiments on the Flow Past Spheres at Very High Reynolds Numbers," *Journal of Fluid Mechanics*, Vol. 54, 1972, pp. 565–575.

[13]Schweyher, H., Lutz, T., and Wagner, S., "An Optimization Tool for Axisymmetric Bodies of Minimum Drag," *2nd International Airship Conference*, Inst. of Static and Dynamics, Stuttgart Univ., Germany, 1996, pp. 203–210.

[14]Lutz, T., Schweyher, H., Wagner, S., and Bannasch, R., "Shape Optimization of Axisymmetric Bodies in Incompressible Flow," *2nd International Airship Conference*, Inst. of Static and Dynamics, Stuttgart Univ., Germany, 1996, pp. 211–224.

[15]Parsons, J., Goodson, R. E., and Goldschmied, R. A., "Shaping of Axisymmetric Bodies for Minimum Drag in Incompressible Flow," *Journal of Hydronautics*, Vol. 8, No. 3, 1974, pp. 100–107.

[16]Upson, R. H., "Metalclad Rigid Airship Development," *Journal of the Society of Automotive Engineers*, Vol. 18, Oct. 1926, p. 128.

[17]Burgess, C. P., *Airship Design*, Ronald, New York, 1927, pp. 1–152.

[18]Brooks, P. W., *Zeppelin: Rigid Airships, 1893-1940*, Putnam, London, 1992, pp. 31, 202, 203.

[19]Pannell, J. R., and Frazer, R. A., "Account of Some Experiments on Rigid Airship R.26," Aeronautical Research Committee, R&M, No. 674, His Majesty's Stationary Office, London, Jan. 1920.

[20]Pannell, J. R., and Frazer, R. A., "Experiments on Rigid Airship R.33," Aeronautical Research Committee, R&M, No. 668, His Majesty's Stationary Office, London, Oct. 1919.

[21]De France, S. J., and Burgess, C. P., "Speed and Deceleration Trials of U.S.S. Los Angeles," NACA TR 318, June 1929.

[22]Pannell, J. R., "Preliminary Experiments on Non-Rigid Airship 'S.S.E.3 100,000' with a Consideration of the Performance of Various Types of S.S. Airship," Aeronautical Research Committee, R&M, No. 693, His Majesty's Stationary Office, London, March 1920.

[23]Taylor, M. J. H. (ed.), *Brassey's World Aircraft and Systems Directory, 1999/2000*, 1999, Brassey's, London, pp. 622, 623.

[24]Arnstein, K., and Klemperer, W., "Performance of Airships," *Aerodynamic Theory*, edited by W. F. Durrand, Vol. 6, Div. R, California Inst. of Technology, Pasadena, CA, 1943, pp. 49–133.

[25]Pannell, J. R., Frazer, R. A., and Bateman, H., "Experiments on Rigid Airship R.32 Part III, Measurements of Resistance and Airspeed," Aeronautical Research Committee, R&M, No. 813, His Majesty's Stationary Office, London, June 1921.

[26]Munk, M. M., "The Drag of Zeppelin Airships," NACA TR 117, 1921.

[27]Thompson, F. L., and Kirschbaum, H. W., "The Drag Characteristics of Several Airships Determined By Deceleration Tests," NACA TR 397, March 1931.

[28]Dorrington, G. E., "Use of Small Lighter-Than-Air Vehicles for Mobile Access to the Upper Canopy," *Selbyana*, Vol. 16, No. 2, 1995, pp. 141–143.

[29]Dorrington, G. E., "Project Hornbill: Use of a Small Electric Powered Helium Airship for Scientific Studies of Tropical Rainforest Canopy," *2nd International Airship Conference*, Inst. of Static and Dynamics, Stuttgart Univ., Germany, 1996, pp. 1–11.

[30]Dorrington, G. E., "Some General Remarks on the Design of Airships," AIAA Paper 99-3915, June 1999.

[31]White, F. M., *Fluid Mechanics*, 4th ed., McGraw-Hill, Singapore, 1999, p. 538.

[32]Owen, P. R., "The Aerodynamics of Aircraft and Other Things," *15th Lanchester Memorial Lecture*, Royal Aeronautical Society, London, 4 May 1972.

[33]Lamb, H., "The Inertia-Coefficients of an Ellipsoid Moving in Fluid," Aeronautical Research Committee, R&M, No. 623, His Majesty's Stationary Office, London, Oct. 1918.

[34]McLemore, H. C., "Wind-Tunnel Tests of a 1/20-Scale Airship Model with Stern Propellers," NASA TN D-1026, Jan. 1962.

[35]Lutz, T., Leinhos, D., and Wagner, S., "Theoretical Investigations of the Flowfield of Airships with a Stern Propeller," International Airship Convention, Airship Association, July 1996.

[36]Rüger, U., Blank, F., and Kröplin, B., "Acquisition of Flight Data such as Drag and Propeller Thrust by a Remote Controlled Solar Airship," AIAA Paper 99-3908, June 1999.

[37]Frazer, R. A., and Simmons, L. F. G., "The Dependence of the Resistance of Bodies Upon Acceleration, as Determined By Chronograph Analysis," Aeronautical Research Committee, R&M, No. 590, His Majesty's Stationary Office, London, June 1919.

[38]Iversen, H. W., and Balent, R., "A Correlating Modulus for Fluid Resistance in Accelerated Motion," *Journal of Applied Physics*, Vol. 12, No. 3, 1951, pp. 324–328.

[39]Higuchi, H., Balligand, H., and Strickland, J. H., "Numerical and Experimental Investigations of the Flow Over a Disk Undergoing Unsteady Motion," *Journal of Fluids and Structures*, Vol. 10, No. 7, 1996, pp. 705–719.

[40]Odar, F., and Hamilton, W. S., "Forces on a Sphere Accelerating in a Viscous Fluid," *Journal of Fluid Mechanics*, Vol. 18, 1964, pp. 302–314.

[41]Potvin, J., Peek, G., and Brocato, B., "New Model of Decelerating Bluff-Body Drag," *Journal of Aircraft*, Vol. 40, No. 2, 2003, pp. 370–377.